Research for evaluating performance of OWC-type Wave Energy Converter "Backward Bent Duct Buoy"

K. Toyota[1], S. Nagata[1], Y. Imai[1] and T. Setoguchi[1]

[1]Institute of Ocean Energy
Saga University,
Honjyo 1 Banchi, Saga-city, Japan
E-mail: toyota@ioes.saga-u.ac.jp

Abstract

In 1986, Masuda proposed a floating wave energy converter with oscillating water column and it was named Backward Bent Duct Buoy (BBDB). In order to design a floating OWC-type wave energy converter such as BBDB optimally, it is necessary to develop a numerical analysis code in time domain on motions of BBDB, air flow in air chamber and rotation of air turbine in waves. As a first step for developing such numerical code, in this paper, first, equations of motion of a floating OWC-type wave energy converter in waves considering memory effect by air pressure in air chamber are shown. Second, some calculation results in frequency domain by 3D boundary element method, which are a base of above calculation in time domain, are shown. Experiments on exciting forces and radiation forces are also carried out and calculation results are compared with experimental results in frequency domain. In addition, BBDB has negative drift force in specific frequency region and it is important to estimate mooring cost for practical use. However, detail on it is still not clear. So, to make it clear experimentally, four kinds of tank tests were carried out and discussed in this research.

Keywords: Backward Bent Duct Buoy, Drift Force, Hydrodynamic Coefficients

1 Introduction

Many types of wave energy converters(WEC) that are based on various concepts have been proposed in recent years (Cruz[1]). Various methods evaluating energy removed from the waves by such converters are also shown (Falnes[2]).

Recently, authors are trying the research with the aim of the practical application of Backward Bent Duct Buoy(BBDB) which is one of floating oscillating water column type WEC. This device was invented by Masuda[3] and consists an air chamber, horizontal duct, buoyancy chamber and turbine as shown in Fig.1 This device has some advantages, that is, i)the primary conversion efficiency is higher than other floating OWCs, ii)as the wavelength for which primary conversion efficiency is maximum is about four times the length of the BBDB, a longer floating structure is not required. iii)as BBDB slowly advances against wave propagation direction in particular wave frequency band, the mooring force and mooring cost are deduced in irregular sea.

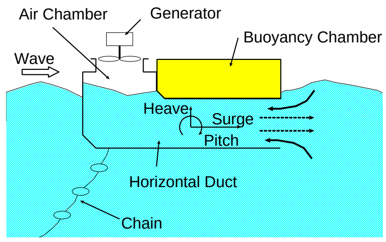

Figure 1: Principle of BBDB

As BBDB has such good characteristics, the research on BBDB has been carried out in Ireland, Korea and Japan. Masuda et al.[4], Lewis et al.[5] and Nagata et al.[6] carried out the wave tank test to make clear the primary conversion characteristics of BBDB.

However, it needs a vast number of tests to make clear the optimal hull shape experimentally. So, it is required that a numerical analysis code (System Simulation) in time domain which can estimate the motion of the floating body and mooring system, the fluctuation of air pressure in the air chamber and the rotational speed of turbine at the same time in irregular waves.

Sarmento et al. [7] and Falcao et al. [8] carried out system simulations that can obtain the free surface elevation distribution of fixed type OWC accurately. Falcao and Justino showed the numerical method in time domain to estimate the total performance considering the air pressure distribution in air chamber and characteristics of turbine. They expressed the radiation air-flow

© Proceedings of the 8th European Wave and Tidal Energy Conference, Uppsala, Sweden, 2009

rate as a convolution integral involving air pressure in air chamber based on the solution in frequency domain.

The system simulation for a floating OWC-type wave energy converter does not yet seem to propose. With regard to the primary conversion efficiency of a floating OWC in frequency domain, Osawa et al.[9] and Hong et al. [10] investigated about Mighty-Whale and BBDB respectively. However, they had not solved the radiation problem concerning the radiation of waves caused by an oscillating dynamic air pressure on the free surface in the air chamber. Therefore they introduced an experimental parameter, which is not easy to determine, on the free surface condition in the air chamber in solving the diffraction problem and the radiation problem by body motion.

In addition, the BBDB has a characteristic that slowly advances in a direction opposite to the wave propagation in some incident wave frequency range. For this characteristic, it seems to reduce the mooring force and the mooring cost in irregular sea. On this advantage, McCormick [11] showed the existence of the negative drift force acting on the BBDB, which acts in a direction opposite to the wave propagation, in some wave frequency range by the tank test. Hong[12] and Kim [13] also showed negative drift force in a tank test, and compared the measured negative drift force with the calculated results based on the potential theory. However, the mechanism of generation of the negative drift force is not clear.

The first purpose of our research is to develop a optimal design method for the floating OWC-type WEC such as BBDB, which doesn't introduce an experimental parameter on the free surface condition, and can take the body motions, the air pressure in the chamber, the free surface elevation in the chamber and characteristics of the mooring system and turbine in waves into account simultaneously. In this method, the fluid motion induced by the air pressure in the chamber is obtained as a solution of radiation problem in frequency domain and the solution in time domain is obtained in terms of convolution integral in the same manner as Falcao. And the second purpose is to make clear the characteristics and the mechanism of generation of the negative drift force acting on the BBDB in regular waves.

In this paper, as the first step to develop a numerical analysis method mentioned above, firstly, equations of motion of a floating OWC-type WEC in waves using the impulse response matrix by body velocity and air pressure in air chamber are deduced.

Secondary, the exiting force by incident wave and radiation force induced by the body motion and the air pressure fluctuation in chamber acting on BBDB are obtained by using three dimensional boundary element method in frequency domain. Nagata et al.[14] carried out the wave tank test for hydrodynamic characteristics of the BBDB. So in this paper, the validity of numerical method were confirmed by comparing with this experimental results.

Furthermore, the characteristics of the negative drift force acting on the BBDB in regular waves are investigated by the two-dimensional wave tank test. Four kinds of experiments are carried out. The first experiment is a usual drift force testing for the BBDB moored by a soft mooring system. The second one is a drift force testing for the fixed BBDB. The third one is a drift force testing for the BBDB whose the surge motion is only possible. The fourth one is a forced pitch oscillation test in which the BBDB is rotated about the center of the air chamber. From these experiments, the mechanism of the generation of negative drift force acting on BBDB is discussed.

2 Fundamental equations for Calculating the Transient Motion of BBDB

In this section, equations of motion of a floating OWC-type wave energy converter in waves using the impulse response matrix by the body velocity and the air pressure in the air chamber are derived. Equations of a floating body in waves using the impulse response matrix by body velocity were already derived by Cummins[15], Oortmerssen[16] and Mei[17]. We shall add the effect of air pressure in air chamber to equations of motion of a floating body which they obtained.

The Cartesian coordinate system is adopted for formulation in this paper. The origin of coordinate system is located on the still water surface, x-axis, y-axis, and z-axis are taken in the longitudinal direction, the lateral direction, and the vertical direction of floating body respectively. Fluid surrounding the floating body is assumed to be incompressible, irrotational and inviscid. Therefore the velocity potential Φ can be defined. The linearized governing equations for Φ are as follows

$$\nabla^2\Phi = 0 \qquad \text{(in fluid)} \quad (1)$$

$$\frac{\partial \zeta}{\partial t} = \frac{\partial \Phi}{\partial z} \qquad \text{(on free Surface,} z=0) \quad (2)$$

$$\frac{\partial \Phi}{\partial t} + g\zeta = 0 \quad (3)$$

(on exterior free surface of BBDB, $z = 0$)

$$\frac{\partial \Phi}{\partial t} + g\zeta = -\frac{P_s}{\rho} \quad (4)$$

(on free surface in air chamber, $z = 0$)

$$\frac{\partial \Phi}{\partial z} = 0 \qquad \text{(on sea bed)} \quad (5)$$

$$\frac{\partial \Phi}{\partial n} = \sum_{\alpha=1}^{6} \dot{X}_\alpha \cdot n_\alpha \qquad \text{(on body surface)} \quad (6)$$

where g is the gravitational acceleration, ζ the free surface elevation, P_s the air pressure in the air chamber, ρ the density of surrounding fluid, n the normal vector which towards the outside of the fluid, and X_α the displacement of the body in the α direction.

2.1 Equations of motion of BBDB in frequency domain

First we summarize the equations of motion of BBDB in frequency domain. Considering time harmonic motions, we write the velocity potential, the displacement of the BBDB and the air pressure in air chamber as

$$\Phi(x,y,z;t) = Re[\phi(x,y,z)e^{-i\omega t}] \tag{7}$$
$$X_\alpha(t) = Re[X_\alpha^a e^{-i\omega t}] \tag{8}$$
$$P_s(t) = Re[P_s^a e^{-i\omega t}] \tag{9}$$

where, i is the imaginary unit, ω the angular frequency, t time, X_α^a the displacement amplitude in the α direction, and P_s^a the amplitude of the air pressure. Re[ ] denotes real part of the complex value. Substituting Eq.(7)$\sim$Eq.(9) into Eq.(1)$\sim$Eq.(6), a following boundary-value problem is obtained.

$$\nabla^2\phi = 0 \quad \text{(in fluid)} \tag{10}$$
$$\frac{\partial\phi}{\partial z} - \frac{\omega^2}{g}\phi = 0 \tag{11}$$
(on external free surface of BBDB,z=0)
$$\frac{\partial\phi}{\partial z} - \frac{\omega^2}{g}\phi = \frac{i\omega}{\rho g}P_s^a \tag{12}$$
(on free surface in the air chamber,z=0)
$$\frac{\partial\phi}{\partial z} = 0 \quad \text{(sea bed)} \tag{13}$$
$$\frac{\partial\phi}{\partial n} = -i\omega\sum_{\alpha=1}^{6} X_\alpha^a \cdot n_\alpha \quad \text{(on the body)} \tag{14}$$

ϕ is decomposed as follows.

$$\phi = \phi_0 + \phi_8 - i\omega\sum_{\alpha=1}^{6} X_\alpha^a\phi_\alpha - \frac{i\omega}{\rho g}P_s^a\phi_7 \tag{15}$$

Above equation, ϕ_0 denotes the velocity potential of the incident wave. In case of deep-water waves, it is given by

$$\phi_0 = \frac{g\zeta}{\omega}e^{kz}e^{i(kx\cos\theta + ky\sin\theta)} \tag{16}$$

where θ is the angle between the incident wave propagation and x axis, k is the wave number. $\phi_1 \sim \phi_6$ are the radiation potentials induced by the motion of BBDB, subscript numbers mean the modes of motion (1:Surge, 2:Sway, 3:Heave, 4:Roll, 5:Pitch, 6:Yaw). ϕ_7 is a radiation potential induced by the fluctuation of the air pressure in the chamber, ϕ_8 is the diffraction potential.

The diffraction potential ϕ_8 is a solution of following boundary-value problem.

$$\nabla^2\phi_8 = 0 \quad \text{(in fluid)} \tag{17}$$
$$\frac{\partial\phi_8}{\partial z} - \frac{\omega^2}{g}\phi_8 = 0 \tag{18}$$
(on external free surface of BBDB,$z=0$)
$$\frac{\partial\phi_8}{\partial z} - \frac{\omega^2}{g}\phi_8 = 0 \tag{19}$$
(on free surface in the air chamber,$z=0$)
$$\frac{\partial\phi_8}{\partial z} = 0 \quad \text{(sea bed)} \tag{20}$$
$$\frac{\partial\phi_8}{\partial n} = -\frac{\partial\phi_0}{\partial n} \quad \text{(on the body surface)} \tag{21}$$
$$(kr)^{1/2}\left(\frac{\partial\phi_8}{\partial r} - ik\phi_8\right) \to 0 \tag{22}$$
$$(kr = k\sqrt{x^2+y^2} \to \infty)$$

The radiation potentials $\phi_\alpha(\alpha = 1 \sim 6)$ satisfy Eq.(17) $\sim$ Eq.(20), and Eq.(22) when ϕ_α is substituted for ϕ_8 in these equations. The boundary condition on the body surface is expressed by the following equation,

$$\frac{\partial\phi_\alpha}{\partial n} = n_\alpha \quad \text{(on body surface)} \tag{23}$$

The radiation potential ϕ_7 induced by the air pressure in the air chamber satisfies Eq.(17),Eq.(18),Eq.(20),Eq.(22) when ϕ_8 is changed into ϕ_7 in these equations. The boundary conditions on the free surface in the air chamber and on the body surface are obtained as follows, which correspond to Eq.(19) and Eq.(20) in the diffraction problem.

$$\frac{\partial\phi_7}{\partial z} - \frac{\omega^2}{g}\phi_7 = -1 \tag{24}$$
(on free surface in air chamber,$z=0$)
$$\frac{\partial\phi_7}{\partial n} = 0 \quad \text{(on body surface)} \tag{25}$$

The forces acting on BBDB in the α direction are expressed by following equations.

$$\begin{aligned} \mathscr{F}_\alpha &= \iint_{S_B} pn_\alpha ds \\ &= F_\alpha^D + F_\alpha^B + F_\alpha^a \end{aligned} \tag{26}$$

where

$$F_\alpha^D = Re[i\rho\omega\iint_{S_B}(\phi_0+\phi_8)n_\alpha ds] \tag{27}$$
$$F_\alpha^B = -\sum_{\beta=1}^{6}\mu_{\alpha\beta}(\omega)\ddot{X}_\beta - \sum_{\beta=1}^{6}\lambda_{\alpha\beta}(\omega)\dot{X}_\beta \tag{28}$$
$$F_\alpha^a = -\gamma_\alpha\dot{P}_s - \sigma_\alpha P_s \tag{29}$$
$$\mu_{\alpha\beta}(\omega) = \rho\iint_{S_B}\mathrm{Re}\phi_\beta n_\alpha ds \tag{30}$$
$$\lambda_{\alpha\beta}(\omega) = \rho\omega\iint_{S_B}\mathrm{Im}\phi_\beta n_\alpha ds \tag{31}$$

$$\gamma_\alpha(\omega) = \frac{\omega}{g}\iint_{S_B}\mathrm{Im}\phi_7 n_\alpha ds \tag{32}$$
$$\sigma_\alpha(\omega) = -\frac{\omega^2}{g}\iint_{S_B}\mathrm{Re}\phi_7 n_\alpha ds \tag{33}$$

Therefore the equations of motion of BBDB in frequency domain is expressed by the following equation.

$$\begin{aligned} &[M_{\alpha\beta} + \mu_{\alpha\beta}(\omega)]\ddot{X}_\beta + [\lambda_{\alpha\beta}(\omega)]\dot{X}_\beta + [C_{\alpha\beta}]X_\beta \\ &+[\gamma_\alpha(\omega)]\dot{P}_s + [\sigma_\alpha(\omega) + S_\alpha]P_s = F_\alpha^D + F_\alpha^m \end{aligned} \tag{34}$$

where F_α^D is the exiting force, $C_{\alpha\beta}$ the buoyancy restoring force coefficients, S_α the restoring force coefficients of air in chamber, F_α^m the resultant forces of the mooring force and wind force etc..

2.2 Equations of Motion of BBDB in time domain

Cummins[15], Oortmerssen[16] and Mei[17] derived the equations of motion in waves using the impulse response matrix by body velocity. We shall add the effect of air pressure in air chamber to equations of motion of a floating body obtained by them.

At first, we assume that a generalized displacement to the body in the α direction and a generalized pressure in the air chamber be given impulsively at the instant $t=\tau$. So that the generalized body velocity and the air pressure are

$$\Delta V_\alpha = V_\alpha(\tau)\delta(t-\tau) \quad , \quad V_\alpha = \dot{X}_\alpha \tag{35}$$
$$\Delta P_s = P_s(\tau)\delta(t-\tau) \tag{36}$$

where δ is Dirac's delta function. Let Φ^Δ be the velocity potential of the radiated waves caused by these impulses. Φ^Δ must satisfy the following boundary value problem.

$$\nabla^2\Phi^\Delta = 0 \qquad \text{(in fluid)} \tag{37}$$
$$\frac{\partial^2\Phi^\Delta}{\partial t^2} + g\frac{\partial\Phi^\Delta}{\partial z} = 0 \tag{38}$$
(on external free surface of BBDB, $z=0$)
$$\frac{\partial^2\Phi^\Delta}{\partial t^2} + g\frac{\partial\Phi^\Delta}{\partial z} = -\frac{1}{\rho}P_s(\tau)\frac{\partial\delta(t-\tau)}{\partial t} \tag{39}$$
(on free surface in chamber, $z=0$)
$$\frac{\partial\Phi^\Delta}{\partial n} = V_\alpha(\tau)n_\alpha\delta(t-\tau) \qquad \text{(on body)} \tag{40}$$
$$|\nabla\Phi^\Delta| \to 0 \tag{41}$$
$$(r=(x^2+y^2)^{1/2}\to\infty\ ,\ t<\infty)$$
$$\Phi^\Delta = 0 \qquad (t<\tau) \tag{42}$$
$$\frac{\partial\Phi^\Delta}{\partial z} = 0 \qquad \text{(on sea bed)} \tag{43}$$

We assume the following decomposition for Φ^Δ.

$$\Phi^\Delta(\mathbf{x},t) = V_\alpha(\tau)\left[\Omega^B_\alpha(\mathbf{x})\delta(t-\tau) + \Gamma^B_\alpha(\mathbf{x},t-\tau)H(t-\tau)\right] + \frac{P_s(\tau)}{\rho}\left[\Gamma^a(\mathbf{x},t-\tau)H(t-\tau)\right] \tag{44}$$

Where H is the Heaviside step function. Substituting Eq.(44) into Eq.(37)$\sim$Eq.(43), the initial-boundary-value problem for Ω^B_α,Γ^B_α and Γ^a can be obtained. Eq.(39) can be transfered as followings. At first, Eq.(45) shows the relation between the Heaviside step function and Dirac's delta function.

$$\frac{\partial H(t-\tau)}{\partial t} = \delta(t-\tau) \tag{45}$$

Since the arbitrary function $h(t)$ satisfies Eq.(46), Eq.(47) can be obtained.

$$h(t)\delta(t) = h(0)\delta(t) \tag{46}$$

$$\dot{h}(t)\delta(t) + h(t)\dot{\delta}(t) = h(0)\dot{\delta}(t) \tag{47}$$

Substituting $\Gamma^a(\mathbf{x},t-\tau)$ for $h(t)$, Eq.(48) can be obtained.

$$\dot{\Gamma}^a(\mathbf{x},t-\tau)\delta(t-\tau) + \Gamma^a(\mathbf{x},t-\tau)\dot{\delta}(t-\tau) = \Gamma^a(\mathbf{x},0)\dot{\delta}(t-\tau) \tag{48}$$

Substituting Eq.(45), Eq.(48) etc. into Eq.(39), a following equation can be obtained.

$$\begin{aligned}
&V_\alpha(\tau)\Big[\Omega^B_\alpha(\mathbf{x})\ddot{\delta}(t-\tau) + \Gamma^B_\alpha(\mathbf{x},0)\dot{\delta}(t-\tau) + \\
&\left\{\frac{\partial\Gamma^B_\alpha(\mathbf{x},t-\tau)}{\partial t} + g\frac{\partial\Omega^B_\alpha(\mathbf{x})}{\partial z}\right\}\delta(t-\tau) \\
&+\left\{\frac{\partial^2\Gamma^B_\alpha(\mathbf{x},t-\tau)}{\partial t^2} + g\frac{\partial\Gamma^B_\alpha(\mathbf{x},t-\tau)}{\partial z}\right\}H(t-\tau)\Big] \\
&+\frac{P_s(\tau)}{\rho}\Big[\Gamma^a(\mathbf{x},0)\dot{\delta}(t-\tau) + \frac{\partial\Gamma^a(\mathbf{x},t-\tau)}{\partial t}\delta(t-\tau) \\
&+\left\{\frac{\partial^2\Gamma^a(\mathbf{x},t-\tau)}{\partial t^2} + g\frac{\partial\Gamma^a(\mathbf{x},t-\tau)}{\partial z}\right\}H(t-\tau)\Big] \\
&= -\frac{P_s(\tau)}{\rho}\dot{\delta}(t-\tau)
\end{aligned} \tag{49}$$

We use the fact that $H,\delta,\dot{\delta}$ and $\ddot{\delta}$ are singularities of different orders, and equate to zero their coefficients individually. Therefore we obtain the following equation from above equation.

$$\Omega^B_\alpha(\mathbf{x}) = 0 \tag{50}$$
$$\Gamma^B_\alpha(\mathbf{x},0) = 0 \tag{51}$$
$$\frac{\partial\Gamma^B_\alpha(\mathbf{x},0)}{\partial t} + g\frac{\partial\Omega^B_\alpha(\mathbf{x})}{\partial z} = 0 \tag{52}$$
$$\frac{\partial^2\Gamma^B_\alpha(\mathbf{x},t-\tau)}{\partial t^2} + g\frac{\partial\Gamma^B_\alpha(\mathbf{x},t-\tau)}{\partial z} = 0 \tag{53}$$
$$\Gamma^a(\mathbf{x},0) = -1 \tag{54}$$
$$\frac{\partial\Gamma^a(\mathbf{x},0)}{\partial t} = 0 \tag{55}$$
$$\frac{\partial^2\Gamma^a(\mathbf{x},t-\tau)}{\partial t^2} + g\frac{\partial\Gamma^a(\mathbf{x},t-\tau)}{\partial z} = 0 \tag{56}$$

Substituting Eq.(44) into Eq.(37),Eq.(38) and Eq.(40)$\sim$Eq.(43), Three kinds of the initial-boundary-value problems for Ω^B_α,Γ^B_α and Γ^a can be obtained. The initial-boundary-value problems for Ω^B_α and Γ^B_α were already shown by Mei[17]. The initial-boundary-value problems for Γ^a is summarized:

$$\nabla^2\Gamma^a = 0 \qquad \text{(in fluid)} \tag{57}$$
$$\Gamma^a = 0 \tag{58}$$
(on external free surface of BBDB, z=0, $t=\tau$) (59)
$$\frac{\partial\Gamma^a}{\partial t} = 0 \tag{60}$$
(on external free surface of BBDB, z=0, $t=\tau$)
$$\Gamma^a = -1 \tag{61}$$
(on free surface in chamber, z=0, $t=\tau$)

$$\frac{\partial \Gamma^a}{\partial t} = 0 \tag{62}$$

(on free surface in chamber,z=0,$t = \tau$)

$$\frac{\partial^2 \Gamma^a}{\partial t^2} + g\frac{\partial \Gamma^a}{\partial z} = 0 \tag{63}$$

(on external free surface of BBDB,z=0,$\tau < t < \infty$)

$$\frac{\partial^2 \Gamma^a}{\partial t^2} + g\frac{\partial \Gamma^a}{\partial z} = 0 \tag{64}$$

(on free surface in chamber,z=0,$\tau < t < \infty$)

$$\frac{\partial \Gamma^a}{\partial n} = 0 \qquad \text{(on body)} \tag{65}$$

$$\frac{\partial \Gamma^a}{\partial z} = 0 \qquad \text{(sea bed)} \tag{66}$$

$$\Gamma^a \to 0 \qquad (|x| \to \infty\,) \tag{67}$$

The above initial-boundary-value problem for Γ^a may be regarded as a radiation problem which determines the fluid motion after the impulsive pressure is applied to the free surface in the air chamber at the instant $t = \tau$. The radiation potential caused by a continuous $V(t)$ and $P_s(t)$ is

$$\begin{aligned}\Phi^R &= \int_{-\infty}^{\infty} d\tau \Phi^{\Delta} \\ &= \Omega^B_\alpha(\mathbf{x})V_\alpha(t) + \int_{-\infty}^{t} \Gamma^B_\alpha(\mathbf{x}, t-\tau)V_\alpha(\tau)d\tau \\ &+ \int_{-\infty}^{t} \Gamma^a(\mathbf{x}, t-\tau)\frac{P_s(\tau)}{\rho}d\tau \end{aligned} \tag{68}$$

The generalized restoring force reacting on the BBDB in the β direction is

$$\begin{aligned} F^R_\beta(t) &= -\rho \iint_{S_B} \frac{\partial \Phi^R}{\partial t} n_\beta ds \\ &= -\mu^B_{\beta\alpha}(\infty)\ddot{X}_\alpha(t) - \int_{-\infty}^{t} K^B_{\beta\alpha}(t-\tau)\dot{X}_\alpha d\tau \\ & -K^a_{\beta 0}P_s(t) - \int_{-\infty}^{t} K^a_\beta(t-\tau)P_s(\tau)d\tau \end{aligned} \tag{69}$$

where

$$\mu^B_{\beta\alpha}(\infty) = \rho \iint_{S_B} \Omega^B_\alpha(\mathbf{x}) n_\beta ds \tag{70}$$

$$K^B_{\beta\alpha}(t) = \rho \iint_{S_B} \frac{\partial \Gamma^B_\alpha(\mathbf{x},t)}{\partial t} n_\beta ds \tag{71}$$

$$K^a_{\beta 0} = \iint_{S_B} \Gamma^a(\mathbf{x},0) n_\beta ds \tag{72}$$

$$K^a_\beta(t) = \iint_{S_B} \frac{\partial \Gamma^a(\mathbf{x},t)}{\partial t} n_\beta ds \tag{73}$$

In deriving Eq.(69), $\Gamma^B_\alpha(\mathbf{x},0) = 0$, which is a equation in a initial-boundary-value problem for Γ^B_α, is used. However, $\Gamma^a(\mathbf{x},0)$ does not equal zero because of Eq.(61). Considering Eq.(69), the equations of motion using the impulse response matrix by body velocity and air pressure in air chamber is

$$\begin{aligned} &\Big[M_{\alpha\beta} + \mu^B_{\alpha\beta}(\infty)\Big]\ddot{X}_\beta(t) \\ &+ \int_{-\infty}^{t} K^B_{\alpha\beta}(t-\tau)\dot{X}_\beta(\tau)d\tau + C_{\alpha\beta}X_\beta(t) \\ &+ (K^a_{\alpha 0} + S_\alpha)P_s(t) + \int_{-\infty}^{t} K^a_\alpha(t-\tau)P_s(\tau)d\tau \\ &= F^D_\alpha + F^m_\alpha \end{aligned} \tag{74}$$

In equations above, F^D_α is exciting force, F^m_α is resultant force caused by mooring system and wind etc.. $K^B_{\alpha\beta}(t-\tau)$ is a retardation function for the motion of the body, $K^a_\alpha(t-\tau)$ is a retardation function for the air pressure in the air chamber. $\mu^B_{\beta\alpha}(\infty)$,$K^B_{\beta\alpha}(t)$ $K^a_{\beta 0}$ and $K^a_\beta(t)$ defined by Eq.(70)~Eq.(73) are calculated by using the solutions of the initial-boundary-value problem for Ω^B_α,Γ^B_α and Γ_a. However, in this paper, we try to represent these values by using the solutions in frequency domain in the same manner as Oortmerssen[16]. At first, we express

$$X_\beta = Re[i\bar{X}_\beta e^{-i(\omega t + \varepsilon_\beta)}] \tag{75}$$

$$P_s = Re[i\bar{P}_s e^{-i(\omega t + \varepsilon_s)}] \tag{76}$$

$$F^D_\alpha + F^m_\alpha = Re[i\bar{F}^{Dm}_\alpha e^{-i(\omega t + \varepsilon_{D\alpha})}] \tag{77}$$

where $\bar{X}_\beta$,$\bar{P}_s$ and $\bar{F}^{Dm}_\alpha$ denote amplitude of X_β,P_s and F^{Dm}_α, ε_β,ε_s,$\varepsilon_{D\alpha}$ are phase of them respectively. Substituting Eq.(75)~Eq.(77) into Eq.(74), the real part of Eq.(74) is expressed as below.

$$\begin{aligned} &\Big[-\omega^2\Big\{M_{\alpha\beta} + \mu^B_{\alpha\beta}(\infty) - \frac{1}{\omega}\int_0^\infty K^B_{\alpha\beta}\sin\omega\tau d\tau\Big\} \\ &\qquad\qquad \times \sin(\omega t + \varepsilon_\beta) \\ &+ \omega\int_0^\infty K^B_{\alpha\beta}(\tau)\cos\omega\tau d\tau \cos(\omega t + \varepsilon_\beta) \\ &\qquad\qquad + C_{\alpha\beta}\sin(\omega t + \varepsilon_\beta)\Big]\bar{X}_B \\ &- \Big[\int_0^\infty K^a_\alpha(\tau)\sin\omega\tau d\tau\cos(\omega t + \varepsilon_s) \\ &\qquad - \Big\{\int_0^\infty K^a_\alpha(\tau)\cos\omega\tau d\tau + (K^a_{\alpha 0} + S_\alpha)\Big\} \\ &\qquad\qquad \times \sin(\omega t + \varepsilon_s)\Big]\bar{P}_s \\ &= \bar{F}^{Dm}_\alpha \sin(\omega t + \varepsilon_{D\alpha}) \end{aligned} \tag{78}$$

On the other hand, substituting Eq.(75)~ Eq.(77) into Eq.(34) which is the equations of motion in frequency domain, the real part of it is expressed as follows.

$$\begin{aligned} &[-\omega^2(M_{\alpha\beta} + \mu_{\alpha\beta}(\omega))\sin(\omega t + \varepsilon_\beta) + \lambda_{\alpha\beta}(\omega)\omega \\ &\qquad \times\cos(\omega t + \varepsilon_\beta) + C_{\alpha\beta}\sin(\omega t + \varepsilon_\beta)]\bar{X}_\beta \\ &+ [\gamma_\alpha(\omega)\omega\cos(\omega t + \varepsilon_s) \\ &\qquad + (\sigma_\alpha(\omega) + S_\alpha)\sin(\omega t + \varepsilon_s)]\bar{P}_s \\ &= F^{Dm}_\alpha \sin(\omega t + \varepsilon_{D\alpha}) \end{aligned} \tag{79}$$

Comparing Eq.(78) with Eq.(79), we can obtain the following equations.

$$K^{B}_{\alpha\beta}(t) = \frac{2}{\pi}\int_0^\infty \lambda_{\alpha\beta}(\omega)\cos\omega t d\omega \quad (80)$$

$$\mu^{B}_{\alpha\beta}(\infty) = \mu_{\alpha\beta}(\omega) + \frac{1}{\omega}\int_0^\infty K^{B}_{\alpha\beta}(t)\sin\omega t dt \quad (81)$$

$$K^{a}_{\alpha}(t) = -\frac{2}{\pi}\int_0^\infty \omega r_\alpha(\omega)\sin\omega t d\omega \quad (82)$$

$$K^{a}_{\alpha 0} = \sigma_\alpha(\omega) - \int_0^\infty K^{a}_{\alpha}(t)\cos\omega t dt \quad (83)$$

$$S_\alpha = -\iint_{S_a} n_\alpha ds \quad (84)$$

In the right-hand side of these equations, $\mu_{\alpha\beta}(\omega), \lambda_{\alpha\beta}(\omega), \gamma_\alpha(\omega), \sigma_\alpha(\omega)$ are defined in Eq.(30) $\sim$ Eq.(33). S_a in Eq.(84) denotes the area of inside walls of the air chamber except the free surface. Therefore the motions of the BBDB is calculated. Firstly the boundary value problem for $\phi_\alpha(\alpha = 1 \sim 6), \phi_7$, and ϕ_8 shown by Eq.(17)$\sim$Eq.(25) are solved. Secondly the obtained solutions are substituted to Eq.(30) $\sim$ Eq.(33) and Eq.(80)$\sim$Eq.(84). Lastly they are substituted into Eq.(74). The transient motions of the BBDB are calculated by solving this equation.

In order to carry out the System Simulation in which the air pressure in air chamber is unknown, it is necessary to estimate the volume flow, which is the sum of radiation volume flow and excitation volume flow, produced by the oscillating internal free surface. The radiation volume flow is calculated the following equation.

$$Q^R(t) = \int_{A_w} \frac{\partial \Phi^R}{\partial z} ds \quad (85)$$

where, A_w is cross section area at the free surface in the air chamber. The excitation volume flow is also calculated in the same manner. To estimate the total performance of floating OWC type wave energy converter such as BBDB in which the motions of BBDB, the air pressure in chamber and the rotating speed of turbine are unknown quantities, the equations of motions of BBDB, the law of thermodynamics in the air chamber and the principle of the conservation of angular momentum of the turbine are needed. We can get the solution to solve these equations simultaneously.

2.3 Evaluation for Hydrodynamic force acting on BBDB in frequency domain

The numerical method in the time domain shown in the previous section needs the hydrodynamic coefficients in the frequency domain. Generally, these values are obtained from the numerical calculation based on the potential theory. However, since BBDB has some edges on the hull shape, it is expected that the damping force acting on BBDB caused by vortex in fluid is generated.

In this paper, firstly we have calculated the exciting force and the radiation force acting on BBDB in frequency domain by using three dimensional boundary element method based on the potential theory. And we have investigated the validity of the numerical method by comparing the numerical results with the experimental results.

2.4 Experimental Apparatus

As the details of experimental apparatus and results for the hydrodynamic force acting on BBDB are shown in the previous paper (Nagata et al[14]), so it is mentioned just about the experimental model and measured data briefly in this paper.

Table. 1 Size and Characteristics of BBDB Test Model

Length	850(mm)
Width	790(mm)
Height	563(mm)
Length of Buoyancy Chamber	600(mm)
Area of Air Chamber	1486.1(cm^2)
Diameter of Orifice	30(mm)
Weight(no ballast)	56.0(kg)

Table 1 shows the dimensions of the BBDB test model. For exciting force, surge, heave and pitch exciting forces were measured. Radiational forces in heave and pitch modes were measured by means of two sensors that are set at bow and stern of the BBDB in the forced oscillation test. Radiation problem caused by the motions of BBDB and diffraction problem shown by Eq.(17)$\sim$Eq.(23) need experimental data in case that the air pressure in the air chamber equals to the atmosphere pressure. So, in this paper, the tank test was carried out without top cover of the air chamber. Experiments were conducted in the wave basin with 65m in length, 5m in breadth, and 7m in depth in Kyushu university.

2.5 Numerical Analysis Code

Numerical analysis code were developed to calculate the hydrodynamic coefficients by using the three dimensional boundary element method. Applying Green's theorem to a radiation or a diffraction potential and to the Green function, the boundary integral equation on the body is

$$\begin{aligned}&\frac{1}{2}\phi(\xi,\eta,\zeta)\\ &= \iint_S \Big[\phi(\xi',\eta',\zeta')\frac{\partial G(\xi',\eta',\zeta',\xi,\eta,\zeta)}{\partial n}\\ &-G(\xi',\eta',\zeta',\xi,\eta,\zeta)\frac{\partial \phi(\xi',\eta',\zeta')}{\partial n}\Big]ds \quad (86)\end{aligned}$$

where $(\xi',\eta',\zeta'),(\xi,\eta,\zeta)$ denote points on the body, G is Green function. In this paper whole fluid domain was divide into two regions that are outer region of the body(Region I) and inner region of the body (Region II) as shown in Fig.2. As waves in our experiments are deep water wave, the following Green function for outer region, which is applicable for infinite water depth, is used.

$$G_1(\xi',\eta',\zeta',\xi,\eta,\zeta) =$$
$$-\frac{1}{4\pi}(\frac{1}{r_1}+\frac{1}{r_2})-\frac{K}{2\pi}\int_0^{\infty}\frac{e^{k(\zeta+\zeta')}J_0(kR)}{k-K}dk$$
$$+\frac{i}{2}Ke^{K(\zeta+\zeta')}J_0(KR) \tag{87}$$

The Green function for inner region is expressed as follows:

$$G_2(\xi',\eta',\zeta',\xi,\eta,\zeta) = -\frac{1}{4\pi r_1} \tag{88}$$

where

$$r_1^2 = (\xi-\xi')^2+(\eta-\eta')^2+(\zeta-\zeta')^2 \tag{89}$$
$$r_2^2 = (\xi-\xi')^2+(\eta-\eta')^2+(\zeta+\zeta')^2 \tag{90}$$
$$R^2 = (\xi-\xi')^2+(\eta-\eta')^2 \tag{91}$$
$$K = \frac{\omega^2}{g} = \frac{2\pi}{\lambda} \tag{92}$$

$J_0(kR)$: Bessel function of the 1st kind

By dividing the boundary surface S in Eq.(86) into discrete panels and approximating ϕ and its normal derivatives in each panel by a constant value, and then considering the boundary condition at the area which connect the region one and region two, we can obtain a system of algebraic equations for $\phi_i(i=1\sim 8)$.

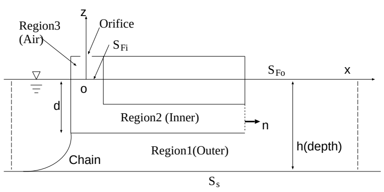

Figure 2: Region for Numerical Analysis

2.6 Numerical and Experimental Results

Exciting Force

In experiments, there is a certain viscous damping in the system. Therefore there is a case in which the calculated value does not agree with experimental one. In order to consider this damping, it seems to be convenient to utilize the artificial damping force due to Rayleigh. If we assume the artificial damping force which is in proportion to the fluid velocity in the duct acts on the fluid, the equations of motion of fluid in each direction are represented as follows.

$$\frac{\partial u}{\partial t} = -\frac{1}{\rho}\frac{\partial p}{\partial x} - \mu u \tag{93}$$
$$\frac{\partial v}{\partial t} = -\frac{1}{\rho}\frac{\partial p}{\partial y} - \mu v \tag{94}$$
$$\frac{\partial w}{\partial t} = -\frac{1}{\rho}\frac{\partial p}{\partial z} - g - \mu w \tag{95}$$

where μ is coefficient for the damping force. Substituting $u = \partial\Phi/\partial x, v = \partial\Phi/\partial y, w = \partial\Phi/\partial z$ into Eq.(93)∼Eq.(95) and take dynamic and kinematic boundary condition into consideration, we can obtain boundary condition for free surface in chamber as follows.

$$\frac{\partial^2\Phi}{\partial t^2} + \mu\frac{\partial\Phi}{\partial t} + g\frac{\partial\Phi}{\partial z} = 0 \tag{96}$$

Substituting Eq.(7) into Eq.(96), we can obtain Eq.(97) as a boundary condition for the diffraction problem considering viscous damping for free surface in chamber in the same way as Eq.(19) is obtained.

$$\frac{\partial\phi_8}{\partial z} - \frac{\omega^2}{g}\Big(1+i\frac{\mu}{\omega}\Big)\phi_8 = 0 \tag{97}$$

The above boundary condition is used in numerical analysis instead of Eq.(19).

Fig.3∼Fig.5 show the Response Amplitude Operator (RAO) of the surge, heave and pitch exciting forces. In these figures, numerical results and experimental results are plotted. Numerical results are for the cases of μ=0, 0.175, 0.2 and 0.3 (1/sec). The vertical axis denotes the exciting forces normalized by density of water ρ, gravity acceleration g, incident wave amplitude ζ_i, displacement ∇ and length of body L. The horizontal axis denotes the wave period. The shortest wave period is 0.73 seconds($\lambda/L = 1.0, \lambda$:wave length) and the longest wave period is 2.86 seconds($\lambda/L = 15.0$) in our experiment. Fig.6 shows RAO of the free surface elevation in the air chamber. In this figure, experimental data are average of values measured at two points by displacement sensor, and numerical results are average of values calculated at 32 panels on the free surface. Numerical results approximately agree with experimental data in these figures.

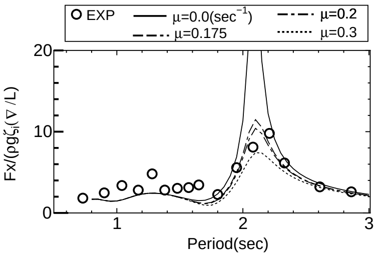

Figure 3: Horizontal Force

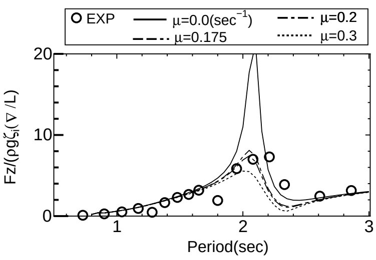

Figure 4: Vertical Force

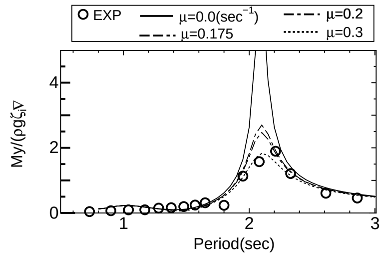

Figure 5: Pitching Moment

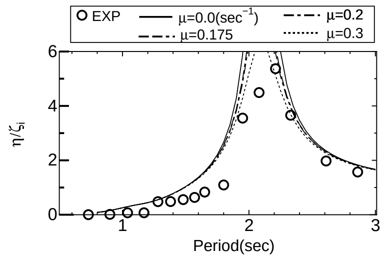

Figure 6: Internal Free Surface Elevation

Radiation Force

Numerical results for radiation force were carried out for three modes of motions (Surge, Heave, Pitch) and forced oscillation of air pressure in the chamber. Forced oscillation tests were carried out only for heave and pitch direction. Fig.7$\sim$Fig.12 show RAO of numerical analysis for the added mass and damping coefficients. Fig.9 and Fig.10 are for the heave mode, and Fig.11 and Fig.12 are for pitch mode, and the experimental results are also plotted in these figures. Numerical analysis results approximately agree with experimental results, but there are difference among them when the wave period is around 2.1 seconds which is natural period of air chamber.

Fig.13 and Fig.14 show RAO of the radiation forces acting on BBDB in the case that the air pressure is applied to the free surface in the air chamber. In these figures, we show two hydrodynamic coefficients. One is a coefficient which is proportion to the time derivative of the air pressure, the other one is a coefficient which is proportion to the air pressure.

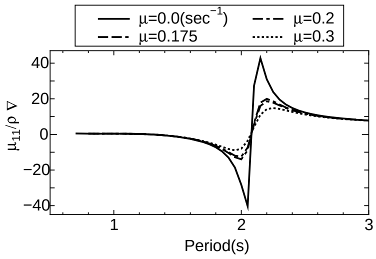

Figure 7: Added Mass Coefficient(surge)

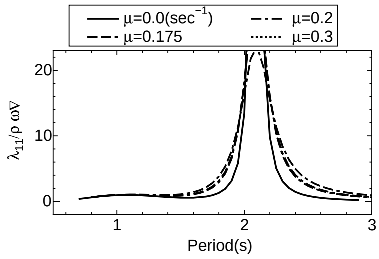

Figure 8: Damping Coefficient (surge)

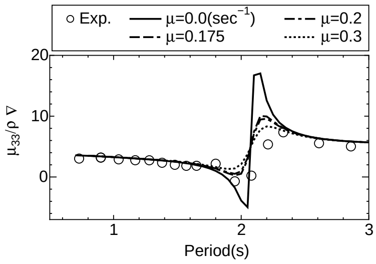

Figure 9: Added Mass Coefficient(heave)

3 Experimental Analysis on Drift Force

3.1 Experimental Apparatus

Experiments for the drift force were carried out in the two-dimensional wave tank in the Institute of Ocean Energy at Saga University. The tank is 19.5m long, 0.8m wide and 1.2m deep. Two active absorbing wavemakers are installed at both ends of the tank. The water depth is 1.0m. BBDB model is same one on the Table.1, and there is an orifice for coming and going of the air flow at the center of the ceiling of the air chamber. The orifice diameter is 30mm or 40mm.

To measure the horizontal drift force acting on the BBDB model, the BBDB model is loosely moored to load cells installed near both ends of the tank by using a light nylon string and rubber bands. Initial tension of the string is about 1.0N. The drift force acting on the BBDB model is defined as the difference between the weather-side force and the lee-side force. To resolve the incident and reflected waves, wave elevation is measured by using four wave gauges installed between the BBDB model and wave generator. The resolution method of incident and reflected waves proposed by Goda [18] is used for this resolution. The drift force is non-dimensionalized

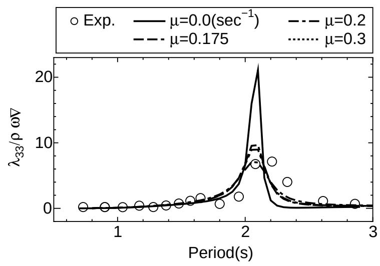

Figure 10: Damping Coefficient (heave)

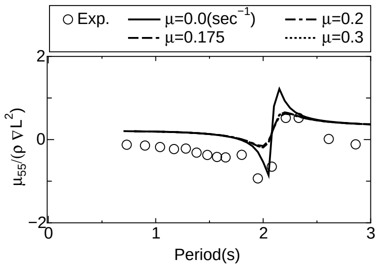

Figure 11: Added Mass Coefficient(pitch)

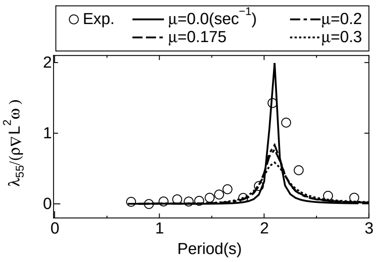

Figure 12: Damping Coefficient (pitch)

by using the amplitude of the incidence wave. The period of the incident regular wave is set from 0.8 to 2.5 second. The ratio of the wavelength (λ) of incident wave and the characteristic length of the BBDB (L=0.85m) is 1.18 to 8.22. The amplitude of the incident wave is almost set as 2.5cm. The motions of the BBDB model in waves are measured by using an image processing method. The image processing system "HALCON" developed by MVTec is used. In addition to the experiments for the drift force acting on the BBDB which was loosely moored, the experiments for the motions of a freely floating BBDB in regular waves were also carried out and the motions of BBDB were measured.

3.2 Drift Force Acting on Loosely Moored Floating Model and Motions of Freely Floating Model

Fig.15 shows the non-dimensionalized drift force acting on the two BBDB model with orifice diameter ϕ of 30mm and 40mm. ρ is the density of water, g the gravitational acceleration, L the length of the BBDB model and ξ_i the amplitude of the incident wave. A positive drift force means that the drift force acts on the BBDB in the direction of the incident wave propagation.

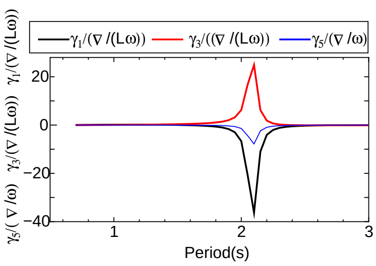

Figure 13: Air Coefficient γ

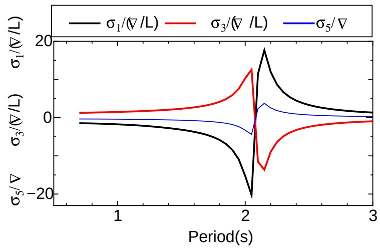

Figure 14: Air Coefficient σ

For the orifice of ϕ=40mm, negative drift force occurs within λ/L=5.0~6.5. For the orifice of ϕ=30mm, it occurred within λ/L=5.3~7.0. Fig.16 shows the amplitude of the surge, heave and pitch motion of the loosely moored BBDB with the orifice of ϕ=40mm in regular waves. Fig.17 shows the surge motions of a freely floating BBDB with the orifice of ϕ=40mm in three regular waves of λ/L=4.0, 5.5, 8.0. In λ/L=4.0, 8.0, the BBDB drifts in the direction of the incident wave propagation with the periodic surge motion by the incident wave. On the contrary, in λ/L=5.5, the BBDB drifts in the direction opposite to the incident wave propagation with the periodic surge motion. Fig.17 shows the attitudes of the freely floating BBDB in time t/T=0, 1/2 for the incident wave of λ/L=5.5 with a wave period T. In the motions of the BBDB, the pitch motion whose center of rotation is almost in the center in the air chamber, is dominant as shown in Fig.18 It is found the followings from Fig.15, Fig.16, Fig.17 and Fig.18.

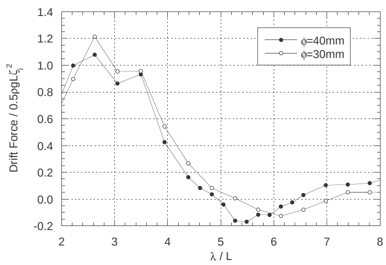

Figure 15: Drift force acting on BBDB (ϕ=30mm, 40mm)

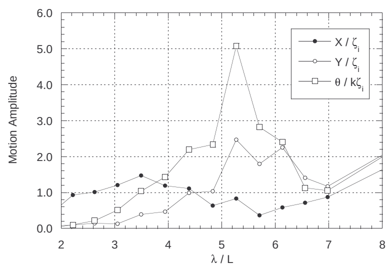

Figure 16: Amplitude of the surge, heave and pitch motions of the loosely moored BBDB with the orifice of ϕ=40mm

(i)In wave frequency range of $\lambda/L < 4$, the surge motion is large, and the heave and pitch motions are rela-

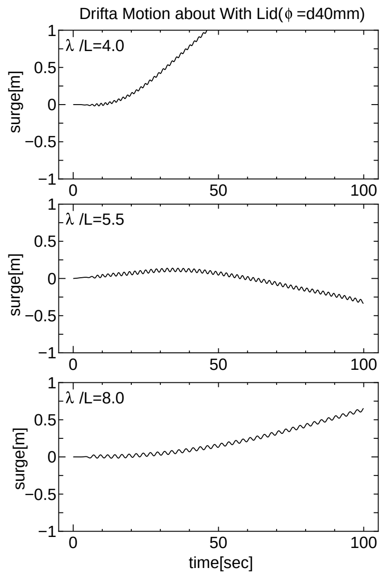

Figure 17: Surge motions of a freely floating BBDB with the orifice of ϕ=40mm in three regular waves of λ/L=4.0, 5.5, 8.0

a) t/T=0 b) t/T=1/2

Figure 18: Attitudes of the freely floating BBDB in time t/T=0, 1/2 (ϕ=40mm)

tively small. Since the drift force acts on BBDB in the wave propagation direction, the freely floating BBDB advances in the wave propagation direction.

(ii)In wave frequency range of λ/L=5∼6.5, the pitch motion, whose the center of rotation is almost in the center in air chamber, is more dominant than other motions. Since the drift force acts on BBDB in a direction opposite to the wave propagation, that is negative drift force, the freely floating BBDB slowly advances in a direction opposite to the wave propagation.

(iii)Since the drift force acts on BBDB in the wave propagation direction in wave frequency range of $\lambda/L >$ 6.5, the freely floating BBDB advances in the wave propagation direction.

3.3 Effect of degree of sealing of air chamber on the drift force acting on BBDB

To examine the effect of the sealing of the air chamber on the drift force acing on the BBDB, the drift forces for two kinds of BBDB models are measured. One is a model of which orifice is sealed, and the other is a model of which lid is detached, that is, the air pressure in the air chamber equals to atmospheric pressure. Fig.19 shows the drift force acting on BBDB for three models of two models mentioned above and the model with the orifice of ϕ=40mm. Fig.20 shows the surge motions of a freely floating BBDB for three BBDB models in regular waves of λ/L=5.5. It is found the followings from Fig.19 and Fig.20.

(i)For the BBDB model with the orifice of ϕ=40mm and one of which lid is detached, the motion of oscillating water column in the L-shaped duct is large and the water is pushed out from the duct to the surrounding fluid. The negative drift force is produced and the freely floating BBDB slowly advances in a direction opposite to the wave propagation. As the stern ascends, a strong vortex grows at the lower end of the duct. This vortex is shed downstream as the stern ascends. (ii)For the model of which orifice is sealed, since the motion of oscillating water column is very small and the water is not pushed out from the duct to the surrounding fluid, the negative drift force does not arise and the freely floating BBDB advances in the wave propagation direction.

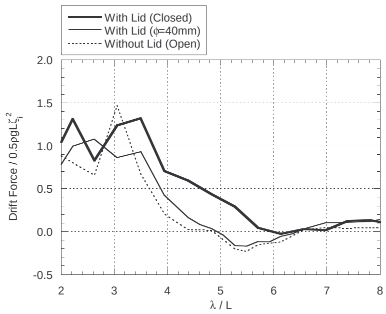

Figure 19: Drift forces for three conditions of air chamber

3.4 Drift Force Acting on Restricted Model

To examine the effect of the motions of the BBDB on the generation of the negative drift force, the drift forces acting on a fixed BBDB model was measured in regular waves. Fig.21 shows the measured drift forces acting on a fixed BBDB model. It is found that the drift force acting on the fixed model, that is, wave drift force, acts on the BBDB model in the wave propagation direction and the negative drift force does not arise.

Next, drift force acting on a BBDB whose surge motion is only possible is measured in regular waves. The heave and pitch motion are restricted by the guide rail on the tank and rollers set in BBDB. Fig.22 shows the measured drift force for this case. In this case, the value of the drift force is positive and the negative drift force does not arise. From these experimental results, it is found that the pitch motion of BBDB is related in the generation of negative drift force.

3.5 Forced Pitch Oscillation Test of BBDB Model

When the negative drift force arises and the freely floating BBDB slowly advances in a direction opposite

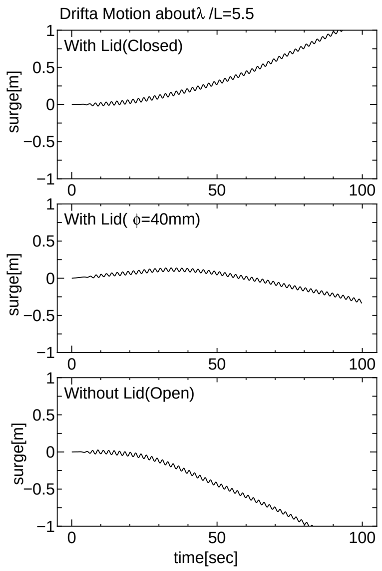

Figure 20: Surge motions of freely floating three kinds of BBDB in regular wave of λ/L=5.5 With Lid (Closed): Model whose orifice is sealed With Lid (ϕ=40mm): Model with the orifice of ϕ=40mm Without Lid (Open): Model whose lid is detached

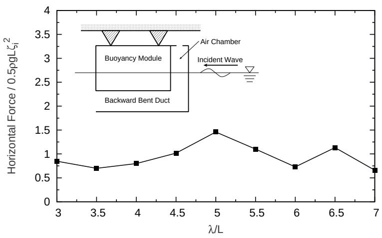

Figure 21: Drift force acting on fixed BBDB

to the wave propagation, the pitch motion whose the center of rotation is almost in the center of the air chamber is more dominant than other motions. Then, whether the thrust arises in the direction of bow of BBDB was examined in the case of forced pitch motion whose center of rotation was the center in air chamber. In this experiment, the amplitude of forced pitch is 2.0 degrees. Fig.23 shows the measured thrust for this case. The thrust has negative value and this means the thrust acts in the direction of bow of BBDB.

3.6 Mechanism of generation of negative drift force

In the frequency ranges in which the negative drift force arises, the wave drift force caused by water wave and the thrust caused by pitch motion of BBDB seems to exist in opposite direction as shown in Fig.24. In order to evaluate these two forces in waves, the drift force acting on BBDB whose surge motion is only possible shown in Fig.22 is compared with the thrust by forced pitch oscillation test shown in Fig.23. Fig.25 compares the drift force in Fig.22 with the thrust in Fig.23 in force unit.

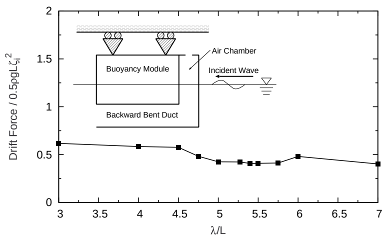

Figure 22: Drift force acting on BBDB whose surge motion is only possible

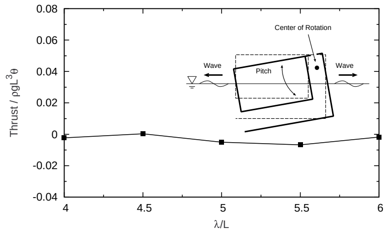

Figure 23: Thrust acting on BBDB by forced pitch oscillation

Since the pitch angle is about 5 degrees in λ/L=4.0∼6.5 in experiments on the drift force shown in Fig.18, 5 degrees are used to calculate the thrust by forced pitch oscillation from Fig.23. From the Fig.25, it is found that the thrust acting on the BBDB by forced pitch oscillation is larger than the drift force, which seems to be the wave drift force, acting on BBDB whose surge motion is only possible. From the these experiments for the drift force acting on the BBDB, the mechanism of the generation of negative drift force acting on BBDB will be considered as follows;

a) Wave drift force acts on the BBDB in the direction of the incident propagation in waves. b) In λ/L=5∼7, pitch motion whose center of rotation is almost in the center in air chamber of the BBDB is generated. c) This pitch motion generates the thrust in a direction opposite to the wave propagation. d) Since this thrust is larger than wave drift force in λ/L=5∼7, the steady force, which is called as negative drift force, as the difference in the thrust and the wave drift force acts on the BBDB in a direction opposite to the wave propagation in this

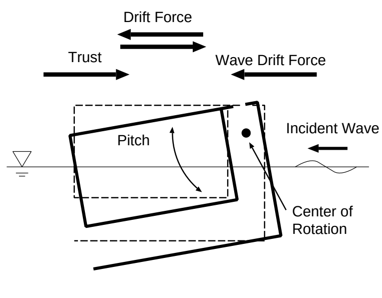

Figure 24: Forces acting on BBDB in regular waves

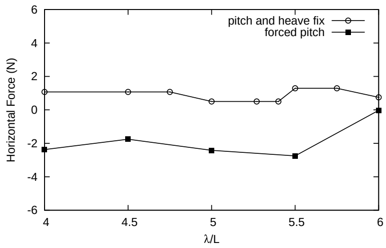

Figure 25: Comparison of drift force acting on BBDB whose surge motion is only possible with thrust by forced pitch oscillation test

frequency range.

4 Concluding Remarks

The purpose of our research is to develop a numerical method in time domain which can evaluate the performance of the floating OWC-type wave energy converters like BBDB with considering the wave-induced motions of body, the air pressure in the air chamber, the free surface elevation in the chamber, characteristics of turbine and mooring system simultaneously.

In this paper, firstly, equations of motion of a floating OWC-type wave energy converter in waves using the impulse response matrix by body velocity and air pressure in air chamber are derived. Secondly, calculation results in frequency domain by three dimensional boundary element method for a diffraction problem and radiation problems by forced motion with unit body velocity and unit air pressure in air chamber for BBDB are shown. In calculation, the numerical results in which the free surface displacement in air chamber is decreased in the natural period by introducing the Rayleigh friction into the free surface condition are also carried out. Experiments on exciting forces and radiation forces for heave and pitch mode are also carried out, and calculation results are compared with experimental results. It is found that numerical results are approximately agree with experimental results,

Furthermore, in order to make the characteristics and the mechanism of generation of the negative drift force acting on the BBDB in regular waves clear, four kinds of experiments are carried out in two-dimensional wave tank. From these experiments, it is found that the negative drift force arises in case that the thrust acting on BBDB in the direction opposite to the wave propagation generated by pitch motion caused by waves is lager than the wave drift force acting on BBDB in the direction of wave propagation.

ACKNOWLEDGMENTS

This work was supported by the Grant-in-Aid for Scientific Research by the Ministry of Education, Science and Culture of Japan and the Collaborative Research Program of Research Institute for Applied Mechanics, Kyushu University.

References

[1] J. Cruz, *"Ocean Wave Energy"*, Springer,2008

[2] J. Falnes,*"Ocean Waves and Oscillating Systems "*, Cambridge University Press, 2002

[3] Masuda Y. Experiences in pneumatic wave energy conversion., *"Utilization of Ocean waves-wave to energy conversion ASCE"*, pp 1–33, 1986

[4] Masuda Y. , Xianguang L. , Xiangfan G. High Performance of Cylinder Float Backward Bent Duct Buoy(BBDB) and its use in European Seas., *"1993 European Wave Energy Symposium"*, pp 323–337, 1993

[5] W.A. Lewis, Gilbaud T. and Holmes B. Modeling the Backward Bent Duct Device -B2D2 A Comparison between physical and numerical models., *"Proceeding of Fifth European Wave Energy Conference "*, pp.54–58, 2003

[6] Nagata S. , Toyota K. , Imai Y. , Setoguchi T. , Kyozuka Y. and Masuda Y. Experimental Research on Primary Conversion of a Floating OWC "Backward Bent Duct Buoy, *"Proceedings of The Fifteenth(2007) International Offshore and Polar Engineering Conference "*, PP.475-482, 2007

[7] A.J.N.A. Sarmento and A. Brito-Melo. An Experiment-Based Time Domain Mathematical Method Model of OWC Power Plants, *"Internatinal Journal of Offshore and Polar Engineering "*, Vol.6 No.3, pp.227–233,1996

[8] A.F. de O. Falcao and P.A.P. Justino, OWC wave energy devices with air flow control , *"Ocean Engineering "*, Vol.26,pp.1275–1295,1999

[9] H. Osawa, Y. Washio, T. Miyazaki, H. Hotta and T. Miyazaki. Primary Convertsion Characteristics of Mighty-Whale , Research and Development of Technology on Wave Energy Utiliztion -Development on Offshore Floting Type Wave Power Device "Mighty Whale", pp.103-112,2004,(in Japanese)

[10] Hong C.D, Hong Y.S. and Hong, W.S. Numerical study on the reverse drift force of floating BBDB wave energy absorber, *"Ocean Engineering "*, Vol.31, pp.1257–1294,2004

[11] M. McCormick and W. Sheehan. Positive Drift of Backward Bent Duct Barge, Journal of Waterway, Port, Coastal, and Ocean Engineering, Vol 118, No.1, 106-111, 1992

[12] D.C. Hong, S. Y. Hong and S. W. Hong. Numerical Study on the Reverse Drift Force of Floating BBDB Wave Energy Absorbers, Ocean Engineering, Vol 31, No 10, 1257-1294, 2004

[13] J.H. Kim and J.M. Lew. An Experimental Study on the Reverse Wave Drift Force of a BBDB Type OWC Wave Energy Device, Proc. of the Fifteenth ISOPE Conference, 2006

[14] Nagata, S., Toyota, K., Imai, Y., Setoguchi Experimental Study on Hydrodynamic Forces acting on a Floating Wave Energy Converter "Backward Bent Duct Buoy",

"Proceedings of The Fifteenth(2008) International Offshore and Polar Engineering Conference ", PP.366-373, 2008

[15] Cummins W.E. The impulse response function and ship motions *"Shiffstechnic"*,Bd.9,Heft 47, pp,101-109.1962

[16] Oocrtmerssen G.Van. The motion of a moored ship in waves *" N.S.M.B. Publication "* No.510, 138p, 1976

[17] Mei C. C. *"Theory and Applications of Ocean Surface Waves"*, John Wiley & Sons. 1983

[18] Y. Goda et al., Estimation of Incident and reflected waves in random wave experiments, Technical note of the port and harbour research institute, No.248, 1-24, in Japanese, 1976